EVLA MEMO 58

USING GRASP8 TO STUDY THE VLA BEAM

Walter Brisken

National Radio Astronomy Observatory

May 9, 2003

Abstract The EVLA will probe the μJy radio universe. Detailed knowledge of the VLA beam will be crucial when taking full advantage of its superb sensitivity. Deep wide-field imaging and mosaicking will require primary beam correction for proper deconvolution and precise polarimetry. The antenna simulation program Grasp8 was used to compute VLA beam patterns in full polarization. Comparison with measurements show encouraging agreement. The quadrupod structure is included in the optics model and suggestions for improvement of its performance are made.

1 Goals of the study

I spent the time from 10 to 26 March, 2003 at the Dominion Radio Astrophysical Observatory (DRAO) near Penticton, B.C., Canada. The main purpose of this visit was to learn to use a software package called Grasp8, a product of Ticra Engineering Consultants [1], and apply it to some VLA optics questions. This included computing the VLA beam shape in full polarization and computing the gain at angles far from bore-sight. During this trip I also investigated the effects of the rectangular cross section quadrupod legs.

The additional goal of learning more about use of Vivaldi arrays as prime focus receivers was also pursued, but will not be discussed here.

2 A VLA model in Grasp8

Grasp8 is an antenna modeling program which uses Physical Optics (PO) and the Physical Theory of Diffraction (PTD) to compute radiation patterns. The PO calculations are carried out by computing induced currents on optical surfaces, which can then be used to compute radiation patterns. This works well for large smooth surfaces, however it breaks down near edges and on small structures (i.e., those with dimensions less than half a wavelength). The surface rims, where the currents in the material have boundary conditions that contradict the PO assumptions, are treated with PTD. Special algorithms are used for the struts which at low frequencies are narrower than one wavelength.

An optics model for the VLA was derived from Figure 1 of EVLA Memo 5 [2]. The rotationally symmetric shape of the primary was provided to Grasp8 as a table of height as a function of radius. The shape of the subreflector is uniquely calculated based on the primary's shape, the placement of the feed, and one point of the subreflector. This asymmetric shape was provided to Grasp8 as a surface tabulated in both x and y. The struts (subreflector support legs) have the cross section of a 28 × 40 cm rectangle with the long side in the radial direction. The struts were truncated at a length of 9.8 m, which is just beyond the height of the subreflector's rim. Figure 1 shows a cut through the model. The tension cables were not included in the optics model. At low frequencies (74 and 330 MHz and to some degree 1.5 GHz), they are probably significant sources of instrumental polarization and increased system temperature. These objects are too small compared to the wavelengths considered to be included in the optics model — Grasp8 is inaccurate for scatterers with dimensions less than about a half wavelength.

The feeds were the only part of the optics that were not fully understood. For most of the calculations (except if noted), a symmetric Gaussian beam with a −12dB taper at 9° feed angle was used. Near field effects for the feed were ignored as the subreflector is in the feed's far field at all frequencies used.

Grasp8 requires its user to explicitly define the calculations to be done. This involves telling it the grid sizes to use on each scattering surface and the order in which to calculate currents and finally describing a grid on which to calculate the radiation pattern. For most calculations (unless otherwise noted) the following
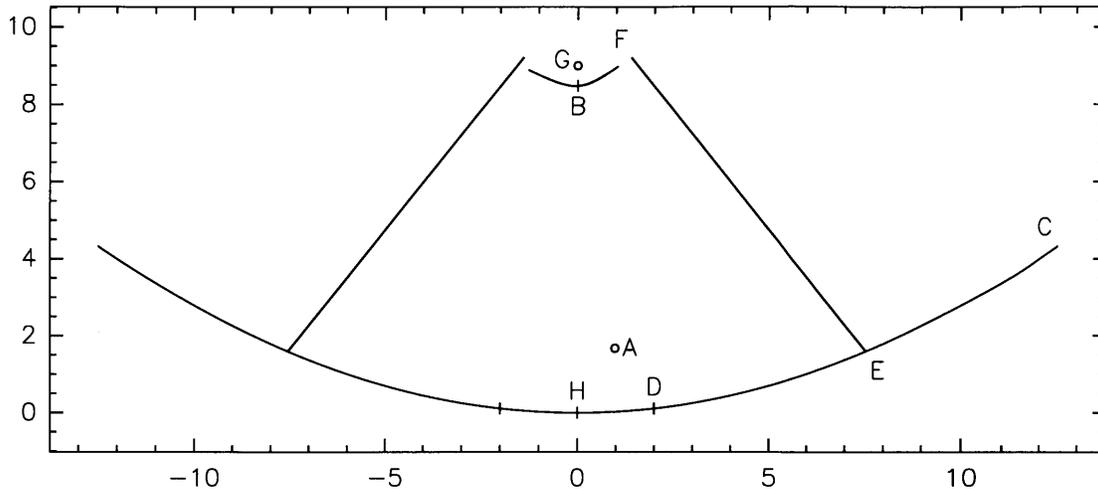
Figure 1: A cross section of the VLA optics model used in Grasp8. The dimensions come from EVLA Memo 5. The coordinates (in meters) for the labeled points are:

Point	Coordinates (meters)
A. Feed	0.975, 1.676
B. Intersection of subreflector and primary axis	0.0, 8.479
C. Edge of primary	12.5, 4.325
D. Inner edge of paneled primary	2.0, 0.112
E. Base of strut	7.550, 1.594
F. Top of modeled strut	1.391, 9.217
G. Prime focus	0.0, 9.0
H. Vertex of primary	0.0, 0.0

scatterings were included, in the order that they are listed. Each line represents illumination of the surface to the right of the arrow by the surface(s) to the left.

$$
\begin{aligned}
\text{Feed} &\rightarrow \text{Sub}_1 \\
\text{Feed}, \text{Sub}_1 &\rightarrow \text{Struts}_1 \\
\text{Sub}_1, \text{Struts}_1 &\rightarrow \text{Primary} \\
\text{Primary}, \text{Feed} &\rightarrow \text{Struts}_2 \\
\text{Primary}, \text{Feed}, \text{Struts}_2 &\rightarrow \text{Sub}_2 \\
\text{Primary}, \text{Feed}, \text{Struts}_2, \text{Sub}_2 &\rightarrow \text{Beam}
\end{aligned}
$$

The subreflector and struts each have two PO objects since scattering occurs twice on each. In these two cases, PO objects 1 and 2 refer to the same scattering surface but contain currents from different scatterings. Each scattering calculation is done in two parts. First the PO calculations are done for the interiors of all surfaces. Then the PTD calculations are done for the object edges (e.g., the edges of the struts and the rims of the primary and subreflector). Grasp8 does not calculate the PTD currents on the destination edge from the PTD currents on the source edge as it is assumed that this contributes a very small amount to the scattered radiation. A future version of Grasp might include this minor effect.

3 Beam polarization

The Grasp8 software package was used to compute the beam of the VLA. At a few different frequencies, the antenna was fed with a pair of orthogonal linear polarized feeds. The (complex) co- and cross-polar beams

2

were then directly computed with Grasp8 out to the third null. The (real-valued) Stokes' parameters can be computed outside Grasp8 by finding the following mean values:

$$I = \langle E_x^2 \rangle + \langle E_y^2 \rangle \tag{1}$$

$$Q = \langle E_x^2 \rangle - \langle E_y^2 \rangle \tag{2}$$

$$U = 2 \langle E_x E_y \cos \delta \rangle \tag{3}$$

$$V = 2 \langle E_x E_y \sin \delta \rangle, \tag{4}$$

where E_x and E_y are the magnitudes of the electric field in the x and y directions respectively. In the expression for U and V, δ is the phase difference between the x and y components of the field. The instrumental polarization is determined by computing these values for an unpolarized source that has been corrupted by the optics. This corruption can be represented by $\mathbf{P}$, the 2×2 complex propagator matrix for the electric field vector. This is determined from the Grasp8 output and consists of elements

$$\mathbf{P} = \begin{bmatrix} \frac{E'_x}{E_x} & \frac{E'_x}{E_y} \\ \frac{E'_y}{E_x} & \frac{E'_y}{E_y} \end{bmatrix}, \tag{5}$$

where the unprimed and primed electric fields represent the uncorrupted and corrupted field respectively.

Since computing time within Grasp8 for a given antenna is roughly proportional to $(\nu \sin \theta_{\max})^4$ due to gridding requirements, simulations were run at the lowest useful frequencies first. The L-band case is special in that the feed is located at $-135°$, which is half-way between two struts, making the optics model exactly symmetric about the plane containing the primary's symmetry axis and the feed. The only effect that could break the symmetry is the gridding done by Grasp8. Thus any asymmetries in the computed beam pattern would be artifacts. Stokes I and U should be symmetric, whereas Stokes Q and V should be antisymmetric, about the diagonal from the top left to the bottom right.

Figure 2 shows the beam's total power pattern (Stokes I) and its fractional instrumental polarization at 1.53 GHz. Subtle differences from the expected symmetry are apparent. The asymmetries were greater when the gridding was coarser. The Q/I and U/I data can be combined to show the magnitude and orientation of the induced linear polarization. Before this was computed, the Q/I data was antisymmetrized and the U/I data was symmetrized as a partial correction to the calculation error. This is shown in Figure 3. The beam patterns for left and right circular polarization are shown in Figure 4. The expected beam squint is visible.

The VLA's beam polarization was measured at 1.4 GHz in 1996 [3]. These measurements are shown in Figure 6. The orientation and magnitude of the calculated fractional circular polarization, V/I agrees well with measurement. The calculated linear polarization is lower than measured by a factor of about two, however has a similar shape. The linear polarization properties were quite sensitive to changes in the antenna model, such as feed taper (especially for slightly asymmetric feeds with non-equal E and H plane patterns), strut location (found out by accident) and gridding. Figures 2 and 3 were made with the symmetric feed pattern and a greatly oversampled grid. Computations made with coarser grids showed greater deviation from the expected symmetry. It is uncertain what the effect on polarization by the VLA L-band lens is. It could contribute to the higher measured polarization.

The VLA beams at 5.0 and 8.4 GHz were also computed, although with less oversampling, which probably causes some of the induced polarization. These are shown in Figures 7 and 8 respectively. Linear polarization plots at these frequencies are not shown since they show suspicious features.

4 Far out beam

The Grasp8 software package was used to simulate a beam pattern of the VLA at 1.5 GHz. A standard feed model was used, which closely approximates a corrugated horn. Results beyond $\theta = 90°$ are probably not reliable. A simulation was also run at 5.0 GHz. Available computation time limited the C-band calculation to 30°. Figures 9 and 10 show the L-band beam out to 100 and 20° respectively. Figure 11 shows the C-band beam out to 30°.
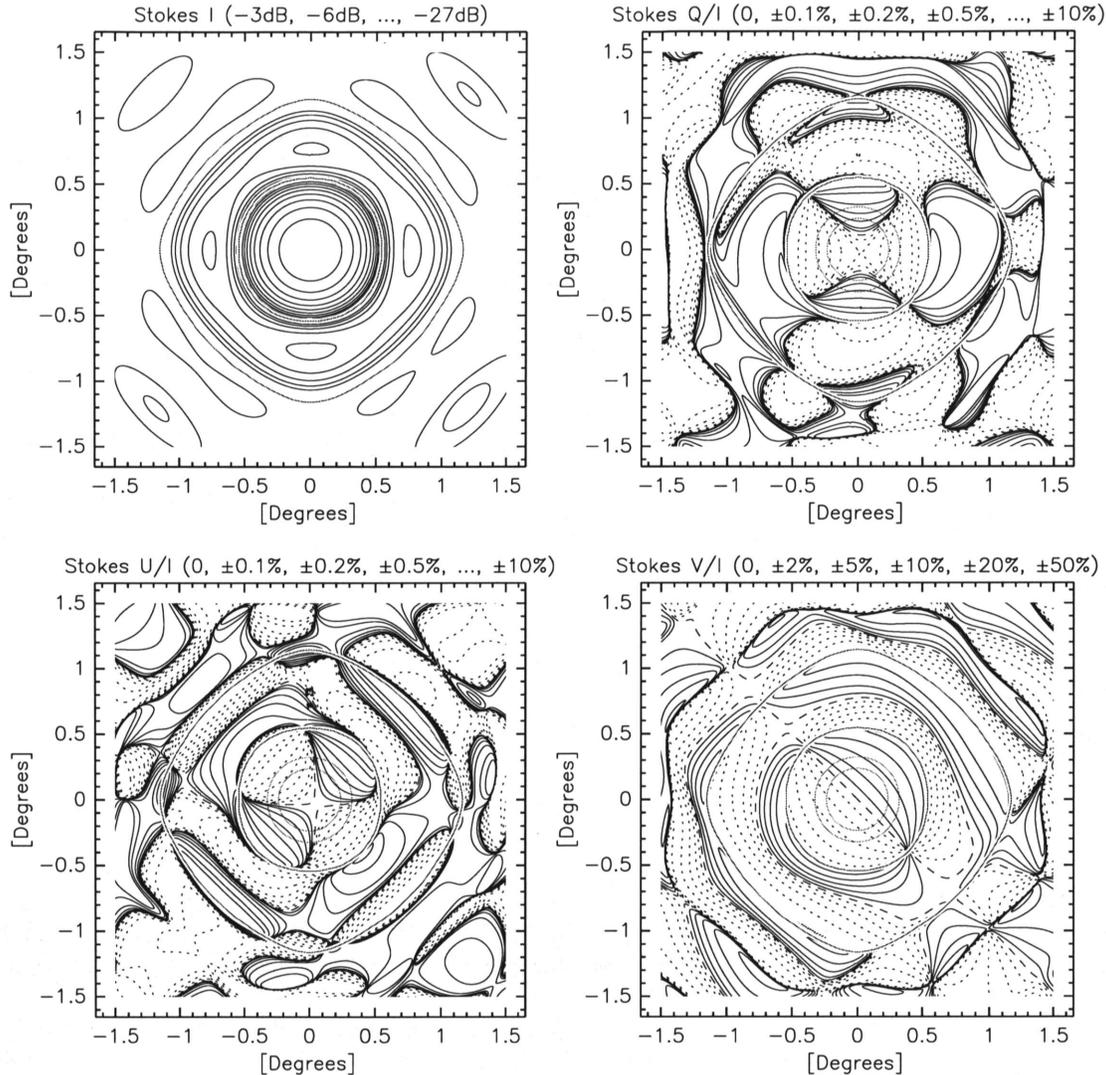
Figure 2: The VLA beam pattern at 1.53 GHz out to the second sidelobe shown in total power (Stokes I) and fractional polarization. The red contours show the first two beam nulls. The green contours show −3dB and −6dB total power. A Gaussian feed with a −12dB taper at 9° feed angle, a good approximation to the EVLA L-band feed, was used. The feed was located at −135° in the feed circle, half way between two struts.

5 Struts

The four struts (quadrupod legs) of a VLA antenna scatter flux in a polarization dependent manner, causing reduced forward gain, increased system temperature, and polarization gradients in the primary beam. For wavelengths much smaller than the width of the struts (roughly X-band and above), the main effect of the struts is the geometric blockage. This comes in two forms: the plane wave blockage of the primary as seen by the source being observed, and spherical wave blockage of the primary as seen by the subreflector. At lower frequencies, the effect of the struts is complicated by diffraction. The induced field ratio (IFR) is a useful measure of effective strut cross section. It is the ratio of the scattering cross section to the geometric cross section. This quantity is polarization dependent. For incident electric fields that are parallel to the strut this ratio, IFR_E, is generally greater than one. For the orthogonal polarization, the ratio IFR_H is generally less
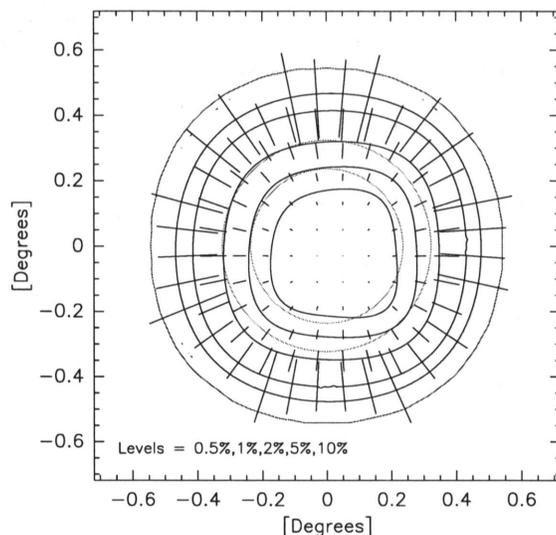
Figure 3: The instrumental linear polarization plotted for the primary beam at 1.53 GHz. The red contour is the first null of the beam. Green contours represent the -3dB and -6dB total power. Black contours represent fractional linear polarization, $\sqrt{Q^2 + U^2}/I$. The line segments show the orientation and magnitude of the excess linear polarization (E vectors). This is derived from the same data used to make Figure 2. The Q and U data were symmetrized before creation of this plot (see text). Note the similarity in shape with the observed linear polarization of Figure 6.

Figure 4: The VLA beam at 1.53 GHz in Left (LL=I-V) and Right (RR=I+V) polarizations. Superimposed on these plots are green contours showing the -3 and -6dB total power contours and red contours showing the first two nulls. Note the beam squint that separates the LL and RR beams. The squint is more easily seen in the 1-D beam cuts of Figure 5. As for Figure 3, the Stokes V data were antisymmetrized before computing the LL and RR beams.

than one. These ratios both tend toward one for wavelengths far less than the strut width. The difference
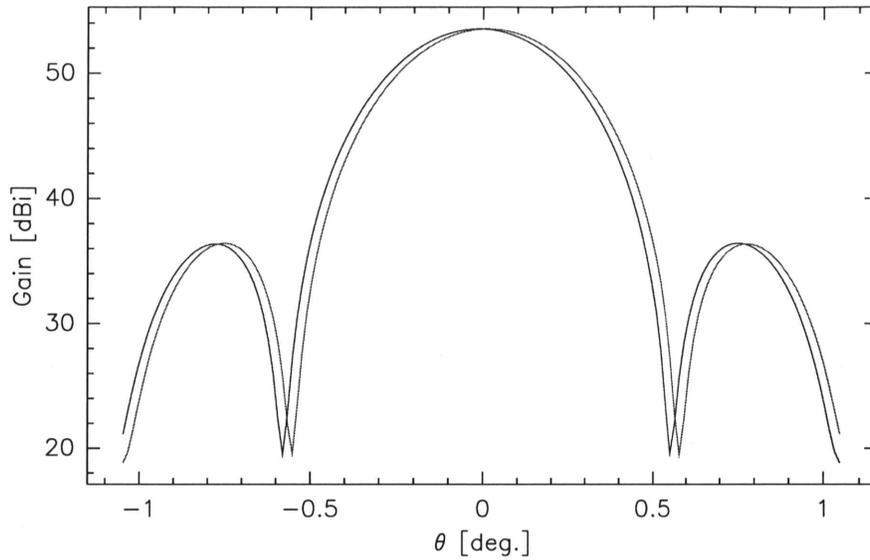
Figure 5: A 1-D diagonal cut through the LL and RR polarized beams of Figure 4 showing the magnitude of the beam squint. At the VLA, the separation between the left and right circular beams is 0.065 times the half-power beam width at any frequency.
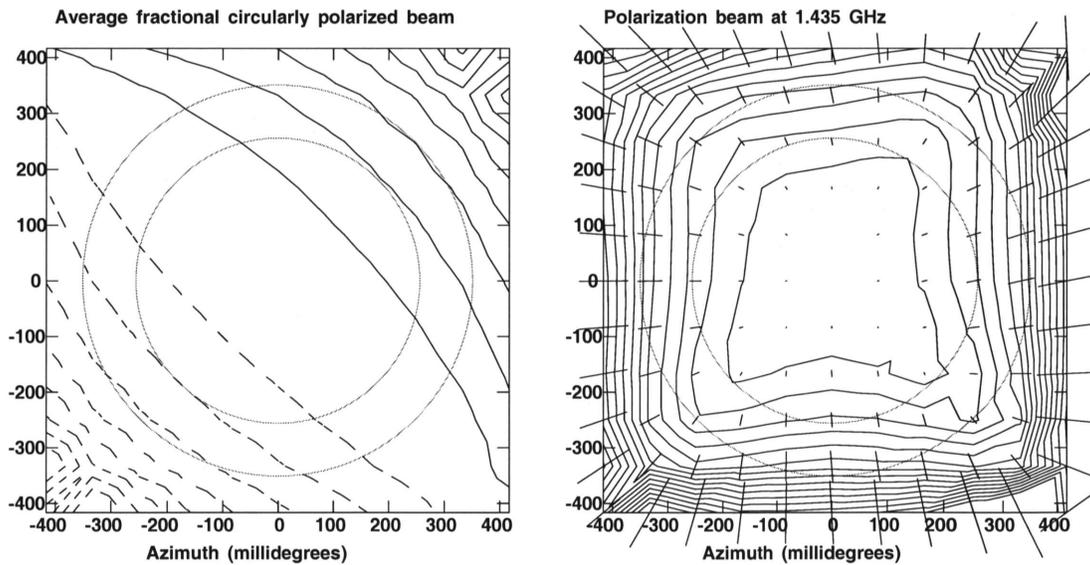

Figure 6: (left) Measured fractional circular polarization beam for the VLA. Contours are shown every 5%. (right) Measured fractional linear polarization for the VLA at 1.435 GHz. Contours are shown each 1%. Dashed contours are negative. Figures from Cotton (1994). Green contours are added at the approximate −3 and −6dB total power levels.

in the IFRs for the two linear polarizations is related to the induced linear polarization, and the average of the IFRs is proportional to the effective blockage.

Teresia Ng as part of her Masters thesis is computing IFRs for different strut cross sections. She has
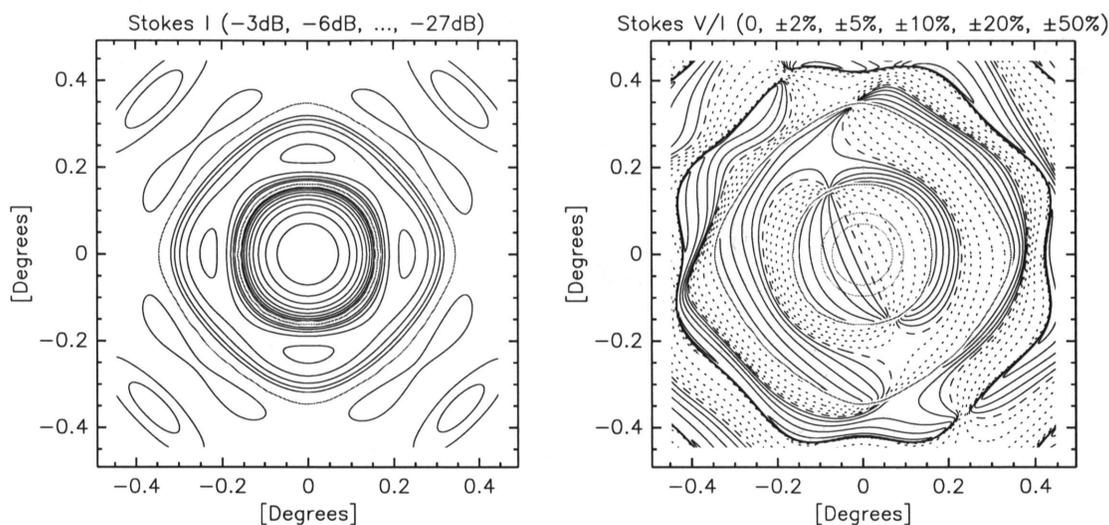
Figure 7: The VLA beam pattern at 5 GHz out to the second sidelobe shown in total power (left) and fractional circular polarization (right). The red contours show the first two beam nulls. The green contours show −3dB and −6dB total power. A feed position angle of 25° was used. Stokes Q and U are not shown since the coarse gridding (required by time constraints) made for suspicious linear polarization plots.
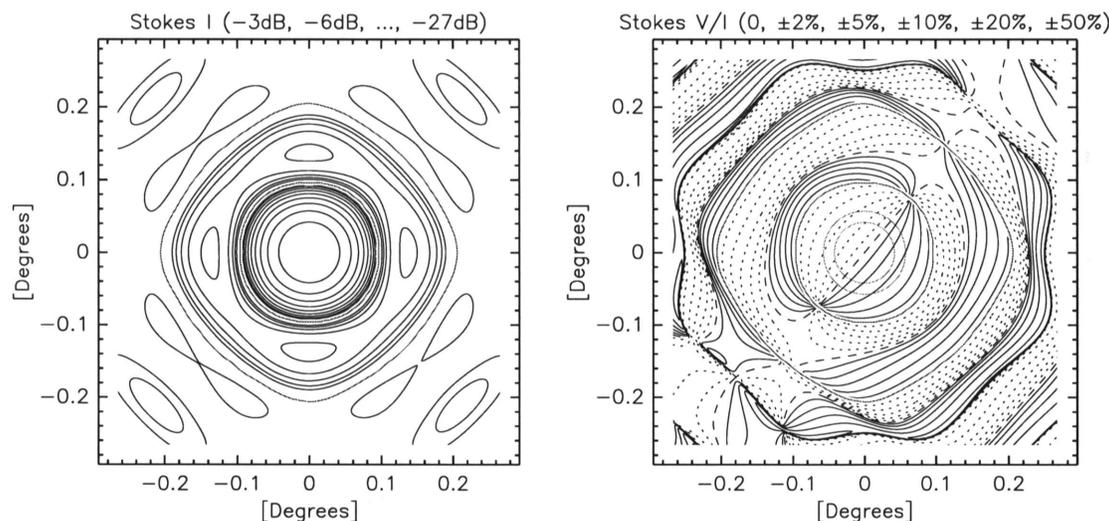

Figure 8: The VLA beam pattern at 8.4 GHz out to the second sidelobe shown in total power (left) and fractional circular polarization (right). The red contours show the first two beam nulls. The green contours show −3dB and −6dB total power. A feed position angle of 140° was used. Stokes Q and U are not shown since the coarse gridding (required by time constraints) made for suspicious linear polarization plots.

concentrated on circular, equilateral triangle, and circle sector shaped struts. Her conclusions suggest that the equilateral triangle with a corner pointing to the antenna interior is the superior structure. She used a software package called Microstripes which integrates in time the currents and electric fields due to an impulsive incident wave. The final outgoing radiation is then Fourier transformed to provide the scattered field for a range of input frequencies.
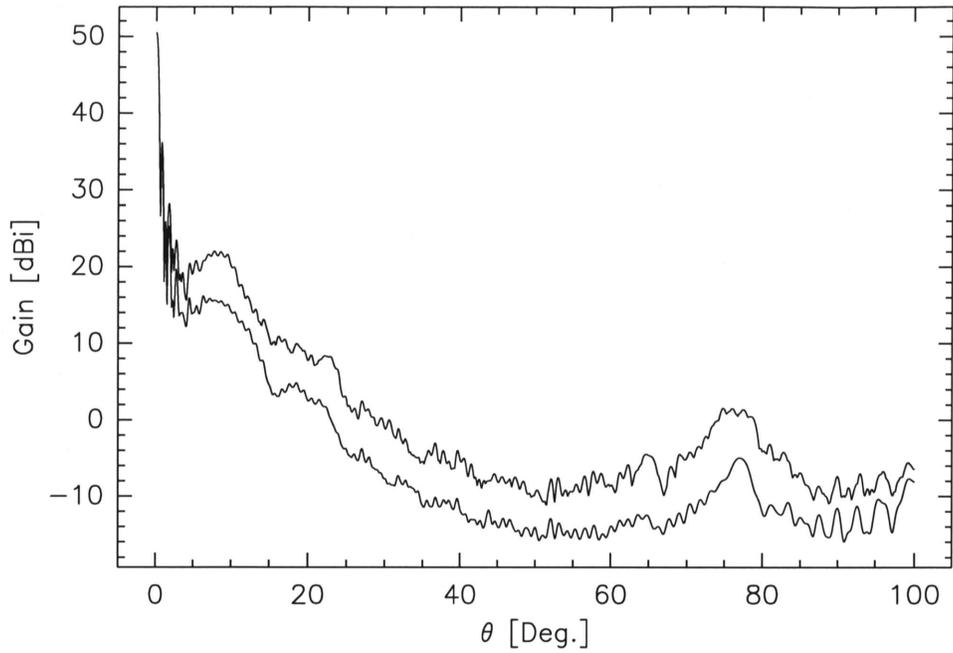
Figure 9: The VLA beam out to 100° from bore-sight. Simulation was done at 1.5 GHz. The bottom curve shows the azimuthally averaged gain at the given value of θ. The top curve shows the maximum gain at the given angle. Note the peaks near 20 and 75° that arise from reflections off the struts. The smooth bump from 5 to 15° comes from feed spillover around the subreflector.
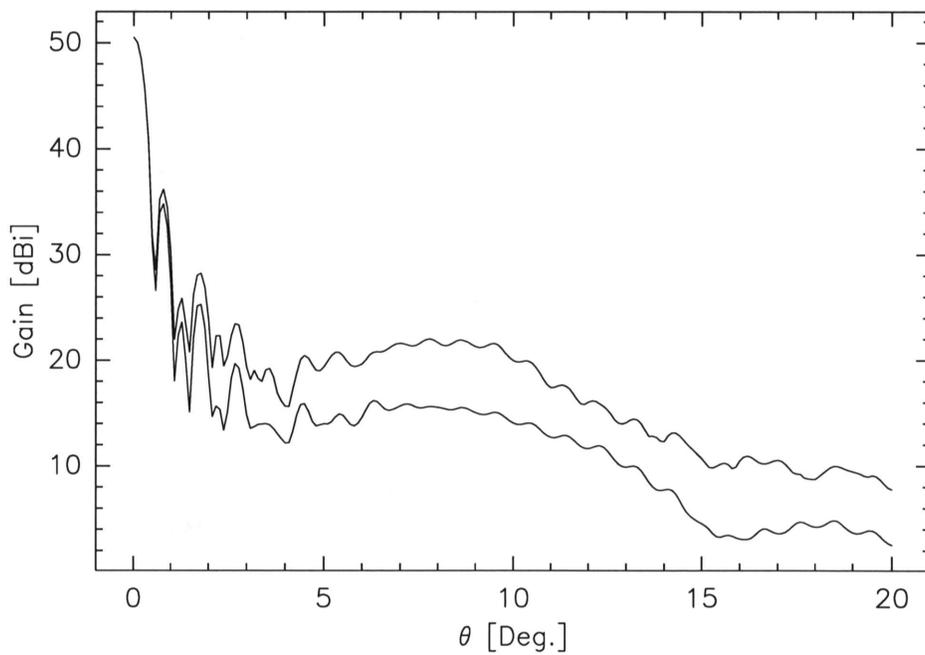

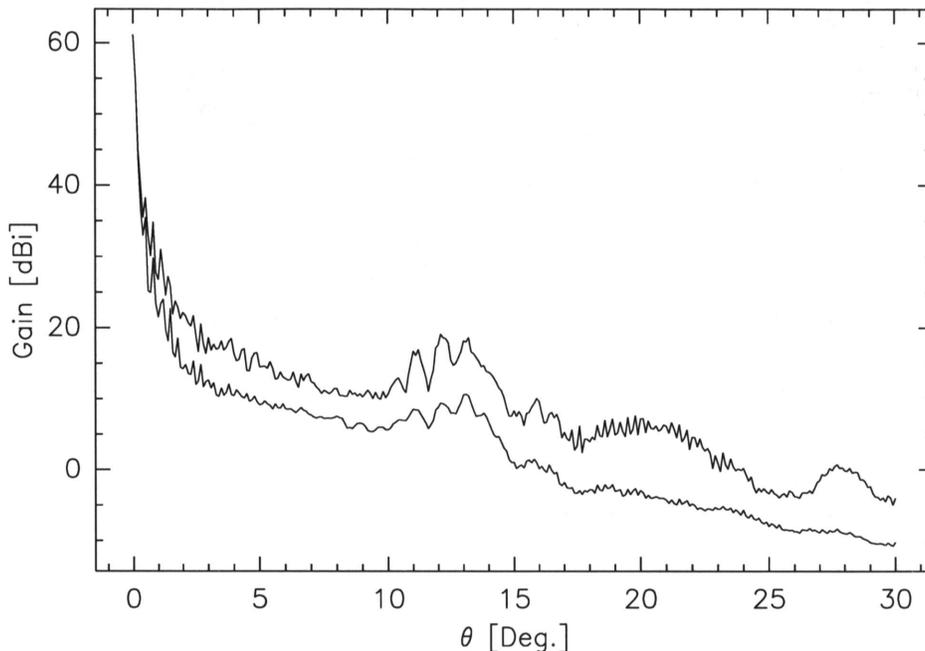Figure 10: Same as Fig. 9, except showing only to $\theta = 20°$.

Figure 11: The VLA beam out to 30° from bore-sight. Simulation was done at 5 GHz. The strut feature is present at 17 to 23° and the feed spillover feature is seen from 11 to 13°.

I used the Method of Moments (MoM) in two dimensions as described in [4] to calculate the IFR for struts with cross sections of a circle, equilateral triangle, rectangle and a rectangle with wedge, among some other, less practical shapes not shown here. The rectangle corresponds to the struts used for the VLA. The circle and triangle calculations agree with those by Teresia Ng. The IFRs for these struts are shown in Figure 12 as a function of cross sectional width in units of wavelength. The equilateral triangle showed the best performance of those tested.

Tom Landecker's earlier study of strut scattering [5] also supports the use of triangular struts. For his paraboloidal antennas, he estimates a reduction of about 3K in system temperature based both on calculation and measurement. VLA beam maps were made with Grasp8 for antenna models with no struts, the current VLA struts, and a modified VLA strut with a wedge on the inside face. The wedges appeared to move the scattered radiation into the more forward direction. Contributions to system temperature due to the unmodified and modified struts were calculated as a function of elevation angle. For zenith angles less than 20° no change was noticed. For zenith angles from 20° to 77° the modified struts showed an average decrease of 0.5K. Beyond 77° the modified struts performed worse by about 0.7K. At these very low elevation angles, this excess system temperature is small compared to that from the feed spillover. It would be instructive to rerun the VLA beam calculations with trianglar struts to determine if additional lowering of the system temperature is possible since the IFR calculations suggest that the triangle shape should be superior.

6   Recommendations

Based on my experience with Grasp8, I would consider it an essential addition to NRAO. It carries a fairly steep (site-wide) price of $35000 plus $5000 per year for updates and (very rapid) technical assistance. Many of the calculations I performed, especially at the higher frequencies, could have benefited greatly from denser gridding, which I could not afford in the time I had. It, or a similar package, will be essential for evaluating modifications to Pie Town and maybe Los Alamos antennas if they are to receive EVLA feeds. It will be useful in the better understanding of the beam polarization which will be needed for high dynamic range
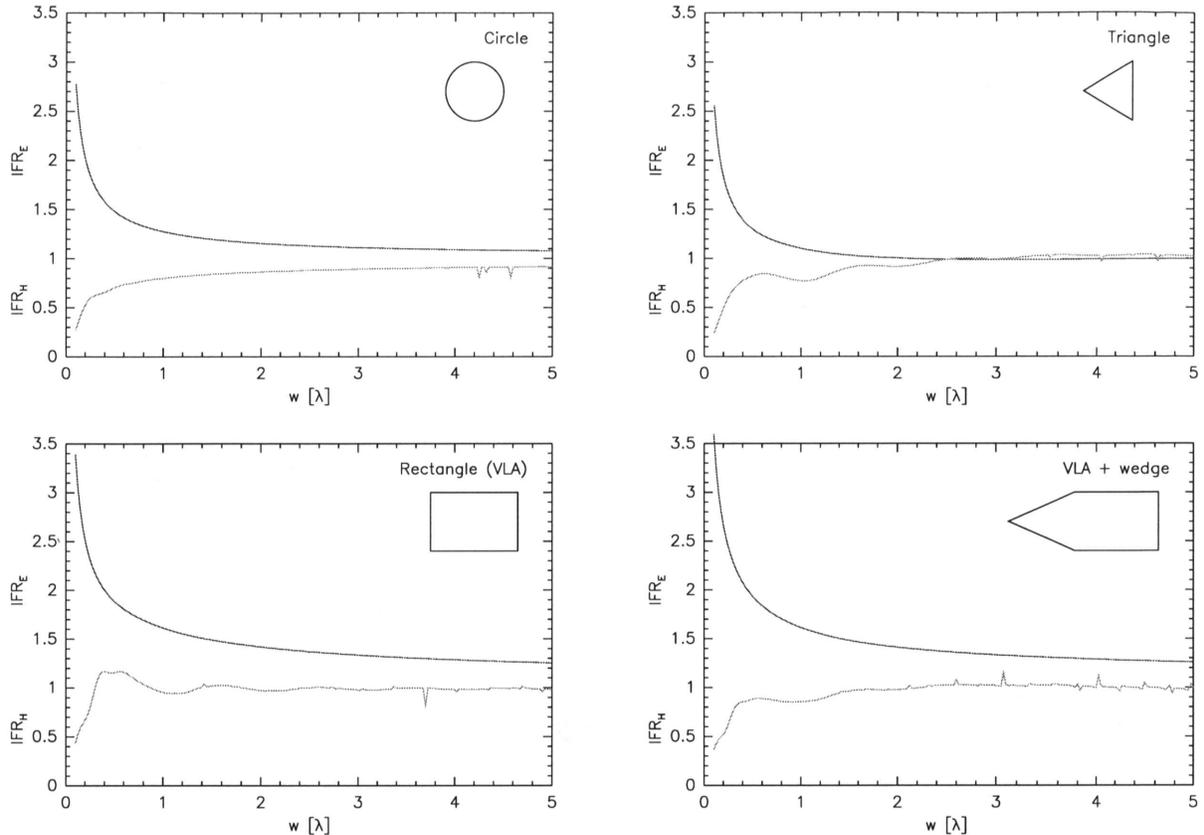
Figure 12: The IFR calculated for 4 cross sectional shaped struts as a function of strut width (in units of wavelengths). The red curves show IFR$_E$ and the green curves show IFR$_H$. Inset are the cross-sectional shapes. The incoming electric field for these shapes approaches from the left. The performance of the equilateral triangle is far superior to any of the other three shapes tested. The spikes in the IFR$_H$ curves are not real — they arise from instabilities in the MoM calculation at certain resonant frequencies.

imaging with ELVA over wide bandwidths. Additionally, it will benefit simulations of the posible EVLA focal plane array.

The performance of struts should be considered when building new antennas for the New Mexico Array. Triangular struts should be considered a better default option than rectangular ones. Even rectangular struts with a wedge pointing inward is likely to reduce system temperature. This last configuration could be tested on the VLA by attaching a folded sheet of aluminum to each strut of one VLA antenna. On a similar note, it would be wise to put some thought into the tension cables, especially if high performance at low frequencies is to be pursued. Unlike for the struts, the tension cables on the VLA are almost parallel to each other, which prevents the cancellation of induced polarization on axis.

7   Summary

Grasp8 has proved to be capable of performing useful beam calculations and would be a great asset for NRAO. Calculated beam patterns agree fairly well with measurements. The discrepancy is likely largely due to the modeled feed pattern differing from the true pattern. Tuning the struts for optimal performance would likeky reduce ground pickup and hence reduce system temperature.

8 Acknowledgments

References

[1] http://www.ticra.com/.

[2] P. J. Napier, "A Larger Subreflector for the VLA", EVLA Memo 5, 1996.

[3] W. D. Cotton, "Widefield Polarization Correction of VLA Snapshot Images at 1.4 GHz", AIPS Memo 86, 1994.

[4] W. V. T. Rusch, et al., "Forward Scattering from Square Cylinders in the Resonance Region with Application to Aperture Blockage", IEEE Transactions on Antennas and Propagation, vol. AP-24, No. 2, March 1976.

[5] T. L. Landecker, "Ground radiation scattered from feed support struts: A significant source of noise in paraboloidal antennas", Radio Science, Vol. 26, No. 2, pp. 363-373, March-April 1991.